Journal of Engineering Mathematics **41:** 33–54, 2001.

Microwave-enhanced chemical vapor infiltration: a sharp interface model

B. S. TILLEY and G. A. KRIEGSMANN
Center for Applied Mathematics and Statistics, Department of Mathematical Sciences, New Jersey Institute of Technology, University Heights, Newark, NJ 07102, U.S.A.

Received 7 August 2000; accepted in revised form 9 April 2001

Abstract. A simple one-dimensional model for describing CVI into a fibrous preform is presented and analyzed. The derivation requires that the thermal and electrical properties of the preform and substrate are disparate. Mathematically the model takes the form of a moving-boundary problem, where the boundary is the interface between the preform and the substrate. Effects of heat loss and radiation at the boundaries and the nonlinear dependence of dielectric parameters on temperature are all taken into account, in addition to the spatial dependence on gas concentration. Processing times for different power levels and inlet concentrations for different initial substrate thicknesses are obtained, and the implications to processing strategies are discussed.

Key words: composites, chemical vapor infiltration, sharp-interface limit, moving boundary problems, microwave heating

1. Introduction

Chemical Vapor Infiltration (CVI) into a fibrous preform has been used to fabricate ceramic composite materials that are mechanically strong and can withstand large operating temperatures. Conventional heating strategies used in this process require large amounts of energy and long processing times. An additional drawback is pore choking at the surface of the preform. This occurs because the surface temperature is hotter than the interior and the concentration of the gas is greater at the surface as well. Thus, the reaction rate is larger at the surface and the pores fill up there, choking off the reaction process in the interior [1]. Optimization of conventional processes has also been the subject of mathematical interest as well [2].

Microwaves, on the other hand, efficiently heat the preform volumetrically and produce an inverted temperature gradient; the surface of the preform is cooler than the interior because of the convective and radiative heat loss. Thus, the reaction rate is higher in the interior of the preform and this causes the composite to grow from the inside out. This configuration results in a more uniform product after the completion of the process. This has been borne out by experiment [3]. However, if this filling process is not done quickly enough, then the pores at the environment/preform interface will close before completion [3].

The use of microwave heating in this particular CVI process has been modeled in a variety of ways. Gupta and Evans [5], and later Deepak and Evans [6, 7], have investigated the microwave heating of the preform assuming that the local electrical and thermal properties of the preform do not change as the reaction proceeds. In this paper, we consider the dynamic version of this process: as the desired product fills the pores, the electrical properties change considerably from the unfilled region. Such property changes in exothermic chemical reactions have been modeled successfully using asymptotic techniques [8, 9, 10]. These techniques rely on a

thin reaction zone (flame front), whose thickness scales on the inverse of the activation energy, in which the chemical process takes place, separating the unreacted zone from the processed region. Appropriate jump conditions in reactant concentration and temperature can be found by analyzing the full reaction system in the reaction zone, and using matched asymptotic expansions to find the appropriate boundary conditions. In a previous work [11], we defined the reacting front as an isotherm in the material, ignoring variations in reactant concentration. We shall see in the current work that these effects are significant, but that the temperature at the interface between composite material and unreacted material remains fixed during the reacting stage of the process. We also show in an Appendix the difference asymptotically between defining the reacting interface thermally or compositionally.

The heating of the preform and substrate, without any chemical reaction, has been performed by Pelesko and Kriegsmann [12]. They found that if the square ratio of the thermal conductivities is proportional to the ratio of the electrical conductivities (this ratio is approximately 10^{-5} for the current system), then the electric and thermal problems decouple. The temperature in the substrate is essentially constant, and the preform temperature obeys a heat equation with a heat flux entering the preform from the substrate that depends on the total power conversion within the substrate and the time rate-of-change of the temperature.

In this paper, we develop a simple one-dimensional model of CVI into a low-loss fibrous preform to fabricate a silicon carbide (SiC) composite. This scenario can occur in two different ways. In the first case a low-loss material, such as alumina (Al_2O_3) can be chosen. In the other, some highly conducting preform material can be used, but its porosity will have to be greater to assume the effective electrical conductivity of the preform remains disparate to that of the composite. In the following, we consider the first case. Since the alumina and SiC have disparate thermal and electrical conductivities the theory presented in [12] is relevant. We extend this model to include a moving front which separates the SiC composite from the preform and develop a numerical method for computing its position as a function of time. Threshold power levels for front propagation are found. We terminate the simulation with a stopping criterion that simultaneously determines when the model loses its asymptotic validity and when the gas inlet pore closes. For lower powers the front moves too slowly and the surface pores close and choke the process. This would produce an unsatisfactory composite. Further, increasing the concentration of the reactant at the inlet also causes the pores to close since the reaction rate depends upon the local reactant concentration.

The paper is organized as follows. In Section 2, we state the physical problem, and using asymptotic techniques find the leading-order problem in of temperature and gas concentration within the preform, and the appropriate boundary conditions local to the moving interface. We simulate the solution to this system numerically in Section 3, and present a parametric study of the process for different power levels, inlet gas concentrations, and initial (uniform) temperatures. We conclude in Section 4 by discussing processing strategies.

2. Problem formulation

2.1. Model

Consider the sample configuration in Figure 1. A plate of SiC of thickness $2\,S_o$ lies between by two layers of a fibrous preform, each of thickness $a - S_o$. The process consists of forcing a trichloromethylsilane (TMS) and (inert) H_2 mixture into both sides of the preform at a fixed

pressure. The typical pore size is on the order of microns, while the thickness of both the substrate and the preform are on the order of centimeters.

The TMS is unstable, and breaks down within the preform into HCl and SiC according to the approximate one-step reaction

$$CH_3Cl_3Si + H_2 + \Delta H_R \rightarrow SiC + H_2 + 3HCl\,, \tag{1}$$

where ΔH_R is the amount of energy per mole (approximately 110 kJ/mole).

The silicon carbide coats the alumina fibers within the preform, filling the pores to generate the composite. The reaction is endothermic, with a reaction rate that has an Arrhenius dependence in temperature and a linear dependence on the local concentration (or equivalently the partial pressure)

$$k_R = k_o \bar{C}_{TMS}\, e^{-\frac{E_a}{R_g T}}\,, \tag{2}$$

where k_o is a rate constant (approximately 2·5 m/s), $\bar{C} = \bar{C}_{TMS}$ is the concentration of the TMS gas, E_a is the activation energy of the reaction (approximately 120 kJ/mole) , R_g is the universal gas constant, and T is the temperature. The sample is assumed to be irradiated by monochromatic electromagnetic plane waves from both sides of the sample. We would like to represent this filling process in a simple mathematical framework in order to gain better insight for enhancements.

A first simplification of the porous preform is to use effective material constants which depend linearly on the local porosity of the material ϕ

$$\rho c_p(\phi) = \rho_A c_{p,A}(1-\phi_o) + \rho_S c_{p,S}(\phi_o - \phi) + \rho_g c_{p,g}\phi\,, \tag{3}$$

$$K(\phi) = K_A(1-\phi_o) + K_S(\phi_o - \phi) + K_g\phi\,, \tag{4}$$

$$\zeta(\phi, T) = \zeta_A(T)(1-\phi_o) + \zeta_S(T)(\phi_o - \phi) + \zeta_g(T)\phi\,, \tag{5}$$

where the subscripts A correspond to the material properties of pure alumina, S to the material properties of pure SiC, and g to the material properties of the gas mixture. The material properties are the density ρ, the specific heat at constant pressure c_p, the thermal conductivity K, and the electrical conductivity ζ. Note that we are assuming the product of the density and heat capacity of the matrix is dependent on the local porosity. In Table 1 we list the density, specific heat (constant pressure), thermal conductivity, electrical conductivity, and thermal diffusivity for alumina Al_2O_3, SiC, and a mixture of H_2 and TMS (10% mole fraction at 1273 K). Notice that the density, heat capacity, thermal and electrical conductivities of the alumina and SiC are several orders of magnitude larger than that of the gas mixture. These terms are then neglected in the following analysis. Also note that the thermal diffusivity of the gas mixture is much larger than that of the alumina fibers, suggesting that the temperature of the gas equilibrates on a much faster time-scale that the thermal conduction of the alumina fibers.

A second simplification is that the porosity of the material can be represented as an array of cylindrical pores (see Sotirchos [4]). Using this geometrical model, we can express the pore radius $\bar{r}(\bar{x}, \bar{t})$ in terms of the local porosity as

$$\left(\frac{\bar{r}}{r_0}\right)^2 = \left[\frac{\log(1-\phi)}{\log(1-\phi_0)}\right]\,, \tag{6}$$

where r_0 and ϕ_0 are the initial values of the pore radius and porosity, respectively. It will be convenient to follow the transition of the composite by tracking the effective pore radius in space and in time, and from this geometric assumption, relate back to the porosity in space.

Table 1. Material properties of alumina, SiC, and the gas mixture at 1273 K and 10 000 Pa. Note that the value of thermal conductivity of the gas mixture is that for hydrogen gas at 273 K.

	Al_2O_3	SiC	H_2 and TMS
ρ (kg/m^3)	3891	3110	0·062
c_p (J/kg K)	1255	1100	0·53
K (W/m K)	7·22	35·7	0·172
σ (mho/m)	0·1	$10^2 - 10^3$	0
κ (m^2/s)	$1{\cdot}5 \times 10^{-6}$	9×10^{-6}	1·28

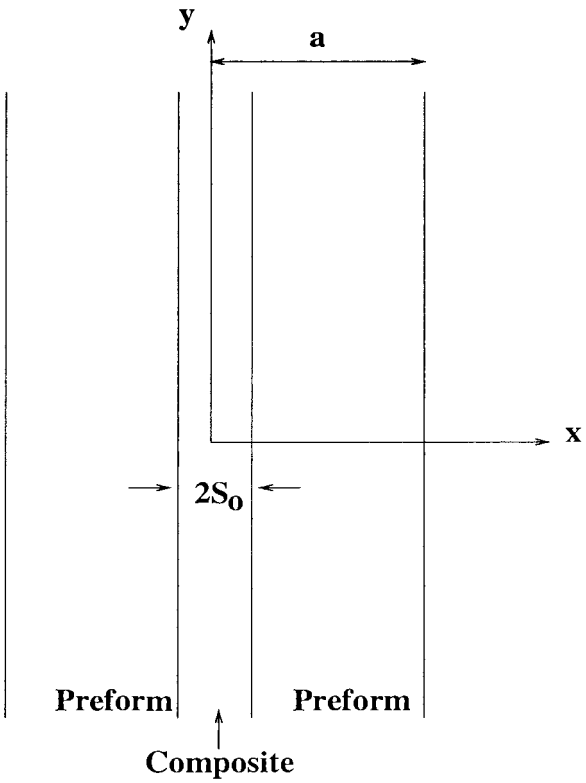

Figure 1. Problem configuration for CVI of a fibrous preform on a composite.

A third assumption is that there is no dependence on the solution in the $\bar{y}$ coordinate. This implies that the model for the gas flow within the porous media can be obtained by considering this gas flow within a single cylindrical pore. However, since the pore radius is on the order of a micron, which is approximately the mean-free-path length scale of the gas molecule, Knudsen diffusion is appropriate (see Gupta and Evans [5], and Skamser *et al.* [13]). The mass flux is related to the concentration gradient and temperature by

$$\Phi_M = -\frac{4\bar{r}}{3}\left(\frac{8R_g T}{\pi M_w}\right)^{1/2}\frac{\partial \bar{C}}{\partial \bar{x}}, \tag{7}$$

where M_w is the molecular weight of the gas. Note that the presence of the reaction requires that there is a mass loss along the inside perimeter of the pore. Further, it is assumed that the filling of the pore occurs in an axisymmetric fashion with respect to the pore axis. A simple conservation of mass argument within a cylindrical pore leads to the following equation for the gas concentration

$$(\bar{r}^2\bar{C})_{\bar{t}} \;=\; \frac{4}{3}\left[\bar{r}^3\left(\frac{8\,R_g\,T}{\pi M_w}\right)^{1/2}\bar{C}_{\bar{x}}\right]_{\bar{x}} - 2\,\bar{r}\,k_R\;. \tag{8}$$

Finally, a simple mass balance across the surface area of the pore gives a relation for the evolution of the pore radius with respect to the reaction

$$\frac{\partial\bar{r}}{\partial\bar{t}} \;=\; -\frac{M_w}{\rho_S}k_R\;. \tag{9}$$

These equations are only valid within the preform $S_0 < |x| < a$. At the interfaces between the preform and the environment, we consider that the concentration of TMS remains fixed at the inlet $\bar{C}(\pm a, t) = C_0$. A second condition in the concentration is needed to close the problem, and we shall derive the appropriate boundary condition in the next section.

Next, we formulate the equations governing the electric field. Two plane, time-harmonic electromagnetic waves of frequency ω impinge upon the sample from the left and from the right. A portion of these waves scatters from the interfaces at $\bar{x} = \pm a$, a portion penetrates to heat the preform, a portion scatters from the interfaces at $\bar{x} = \pm S_0$, and a portion penetrates to heat the substrate. Since the waves impinge the sample symmetrically, we apply the 'no-flux' boundary condition on the electric field at $\bar{x} = 0$. In the free-space region given by $|\bar{x}| > a$, the electric field is given by

$$\mathbf{E} \;=\; E_0\left[\mathrm{e}^{\mathrm{i}\,\bar{k}_0\,\bar{x}-\mathrm{i}\omega\bar{t}} + \Gamma\mathrm{e}^{-\mathrm{i}\,\bar{k}_0\,\bar{x}-\mathrm{i}\,\omega\bar{t}}\right]\mathbf{k} + \text{c.c.}\;, \tag{10}$$

where E_0 is the strength of the incident field, $\bar{k}_0 = \omega/c$, c is the speed of light in free space, Γ is the total reflection coefficient and c.c. is the complex conjugate term.

The electric field is given by $\mathbf{E} = \left[\bar{E}(\bar{x})\,\mathrm{e}^{-\mathrm{i}\omega\bar{t}}\right]\mathbf{k}$, where $\bar{E}$ is its complex amplitude. With these assumptions, Maxwell's equations reduce to the following differential equation

$$\frac{\mathrm{d}^2\bar{E}}{\mathrm{d}\bar{x}^2} + \left(\bar{k}(\phi)\right)^2\left[1 + \mathrm{i}\,\frac{\zeta(\phi,T)}{\omega\epsilon(\phi)}\right]E \;=\; 0\;, \tag{11}$$

where $\epsilon(\phi)$ is the effective permittivity of the medium. The magnetic permeabilities of both materials are assumed to be identical to that of free space.

At the interface $\bar{x} = \pm a$, the tangential electric and magnetic fields are continuous, hence $\bar{E}(\bar{x})$ and its derivative are also continuous at $\bar{x} = \pm a$. This allows us to solve for Γ in terms of the field and its derivative to find that $\bar{E}$ satisfies the boundary condition

$$\frac{\mathrm{d}\bar{E}}{\mathrm{d}\bar{x}} \pm \mathrm{i}\bar{k}(\phi)\bar{E}(\mp a) \;=\; \pm 2E_0\,\mathrm{i}\,\bar{k}_0\,\mathrm{e}^{\mp\mathrm{i}\,\bar{k}_0\,a}\;. \tag{12}$$

Finally, we need to consider the energy balance. There will be a heat-source term that represents the conversion of electrical energy to thermal energy, and a heat-sink term that represents the losses due to the reaction, that is, the temperature T satisfies

$$\left[\rho(\phi)c_p(\phi)T\right]_{\bar{t}} \;=\; \left[K(\phi)T_{\bar{x}}\right]_{\bar{x}} + \frac{1}{2}\zeta(\phi,T)|\bar{E}|^2 - \Delta H_R\,S_A\,k_R\;, \tag{13}$$

where S_A is the surface area available in the preform for the reaction to occur. From Sotirchos [4], this term can be written as

$$S_A \;=\; -\frac{2\bar{r}\,\log(1-\phi_0)}{r_0^2}[1-\phi_0]^{(\bar{r}/r_0)^2}\,, \tag{14}$$

with the symmetry boundary condition given by $T_{\bar{x}} = 0$ at $\bar{x} = 0$.

At the preform/environment interface $\bar{x} = \pm a$, we assume that there are heat loss terms due to advection and radiation

$$K(\phi)T_{\bar{x}} \;=\; -h(T-T_a) - s\epsilon(T^4 - T_a^4)\,, \tag{15}$$

where T_a is the ambient temperature, h is the heat transfer coefficient (approximately 170 W/m^2 K), s is the Stefan-Boltzmann constant, and ϵ is the emissivity.

We nondimensionalize this system by introducing the space scale $\bar{x} = a\,x$, the time scale $\bar{t} \;=\; t\,a^2/\kappa(0)$, where $\kappa(\phi) \;=\; K(\phi)/\rho c_p(\phi)$ and the dimensionless dependent variables $T \;=\; T_a(\theta+1)$, $\bar{C} \;=\; C_0\,C$, $\bar{E} \;=\; E_0 E$, $\bar{r} \;=\; r_0\,r$, and $S \;=\; S_0/a$ to arrive at the following nondimensional system

$$\left\{\frac{\rho c_p(\phi)}{\rho c_p(0)}\theta\right\}_t \;=\; \left[\frac{K(\phi)}{K(\phi_0)}\theta_x\right]_x + \frac{K(\phi)}{K(0)}\,B\,P\,\frac{\zeta(\phi,\theta)}{\zeta(0,0)}|E|^2 - 2\mathcal{K}_R Q r\left[1-\phi_0\right]^{r^2-1/4} C\mathrm{e}^{-\frac{A}{(\theta+1)}}\,, \tag{16}$$

$$\left[r^2 C\right]_t \;=\; D\left[r^3\sqrt{(\theta+1)}C_x\right]_x - 2\mathcal{K}_R r\,C\,\mathrm{e}^{-\frac{A}{(\theta+1)}}\,, \tag{17}$$

$$\frac{\mathrm{d}^2E}{\mathrm{d}x^2} \;+\; \left(\bar{k}(\phi)\,a\right)^2\left[1+\mathrm{i}\nu(r,\theta)\right]E = 0\,, \tag{18}$$

$$\frac{\partial r}{\partial t} \;=\; -M\;\mathcal{K}_R\,C\,\mathrm{e}^{-\frac{A}{(\theta+1)}}\,, \tag{19}$$

where the wavenumber of the electric field in the medium $k(\phi) \;=\; a\,\bar{k}(\phi)$ and the loss term $\nu(\phi,\theta) = \zeta(\phi,\theta)/[\omega\epsilon(\phi)]$. This system is subject to the boundary conditions

$$x = 0: \qquad \theta_x = 0\,, \qquad \frac{\mathrm{d}E}{\mathrm{d}x} = 0\,, \tag{20}$$

$$x = 1: \frac{K(\phi)}{K(\phi_0)}\theta_x = -B\theta - B\,R\,\left[(\theta+1)^4 - 1\right],\ \frac{\mathrm{d}E}{\mathrm{d}x} - \mathrm{i}\,k(\phi)\,E = -2\,\mathrm{i}\,k^{-\mathrm{i}\,k}\,, \tag{21}$$

$$C = 1\,. \tag{22}$$

The nondimensional parameters are given by a Biot number $B \;=\; h\,a/K(\phi_0)$, a measure of input power $P \;=\; (a\zeta(0,0)|E_0|^2)/(2\,h\,T_a)$, the ratio of the thermal diffusion time-scale to the reaction time scale $\mathcal{K}_R = (k_0 a^2)/(r_0\kappa(0))$, a heat of reaction parameter Q, and a ratio of the thermal-diffusion time scale to the gas-diffusion time scale D,

$$Q = C_0\,\frac{[(1-\phi_0)^{1/4}\Delta H_R\,\log(1-\phi_0)^{-1}]}{\rho c_p(0)T_a}\;\;,\;\; D = \frac{4\,r_0}{3\,\kappa(0)}\left[\frac{8\,R_g\,T_a}{\pi M_w}\right]^{1/2}. \tag{23}$$

There is also a mass ratio $M = M_w C_0/\rho_S$, an activation energy $A = E_a/(R_g T_a) \approx 50$, and a radiation heat-loss parameter given by $R = (s\epsilon T_a^3)/h$.

2.2. SHARP-INTERFACE LIMIT

We notice that the activation energy parameter $A \gg 1$. Large activation energy asymptotics have been used successfully in a wide range of problems involving chemical reactions [8, 9, 10]. Since the activation energy is large, we assume that $A = \mathcal{A}/\delta$, where $\delta \ll 1$ is the small parameter scale about which we want to perform an asymptotic expansion. In these chemical-reaction models, a critical temperature θ_c below which the reaction does not occur is defined by the conservation of energy equations local to the reaction zone. A balance of the jump in heat flux across this zone and the heat of reaction within this region (see equation (30) below) suggests a reaction temperature given in terms of the parameters $\mathcal{K}_R$ and Q by

$$Q\,\mathcal{K}_R = \delta \mathrm{e}^{\frac{A}{\theta_c+1}}. \tag{24}$$

Using the values of $a = 1$ cm , $\mathcal{K}_R = 1{\cdot}66 \times 10^8$, $Q = 5 \times 10^{-4}$, $\delta = 0{\cdot}08$ and $r_0 = 1\ \mu$m, we find that $\theta_c = 2{\cdot}589$, which corresponds to a dimensional temperature of $T_c = 1100$ K.

We then define the following unit-order parameters as

$$Q = \delta^2 \mathcal{Q}\ ,\ \ \mathcal{D} = \delta D\ ,\ \ M = \delta^2 \mathcal{M}\ , \tag{25}$$

and rewrite the field equations (16)–(19) as

$$\left\{\frac{\rho c_p(\phi)}{\rho c_p(0)}\theta\right\}_t = \left[\frac{K(\phi)}{K(0)}\theta_x\right]_x + \frac{K(\phi_0)}{K(0)} B\,P\,\frac{\zeta(\phi,\theta)}{\zeta(0,0)}|E|^2 - 2\mathcal{Q}\,r\left[1-\phi_0\right]^{r^2-1/4} C \mathrm{e}^{\frac{\mathcal{A}}{\delta}\left[\frac{1}{(\theta_c+1)}-\frac{1}{\theta+1}\right]}, \tag{26}$$

$$\left[r^2 C\right]_t = \frac{\mathcal{D}}{\delta}\left[r^3\sqrt{(\theta+1)}C_x\right]_x - \frac{2}{\delta^2} r\,C\,\mathrm{e}^{\frac{\mathcal{A}}{\delta}\left[\frac{1}{(\theta_c+1)}-\frac{1}{(\theta+1)}\right]}, \tag{27}$$

$$\frac{\mathrm{d}^2 E}{\mathrm{d}x^2} + k^2(\phi)\left[1+\mathrm{i}\nu(\phi,\theta)\right]E = 0\,, \tag{28}$$

$$\frac{\partial r}{\partial t} = -\mathcal{M}\,C\,\mathrm{e}^{\frac{\mathcal{A}}{\delta}\left[\frac{1}{(\theta_c+1)}-\frac{1}{\theta+1}\right]}. \tag{29}$$

Since the reaction occurs on a much faster time scale than heat diffuses, we note when the reaction temperature occurs, the space scale in which reaction takes place is $O(\delta)$. This suggests that in the limit $\delta \to 0$, this region will, to leading order, be a sharp interface between the composite ($r = 0$) and the preform $r = 1$. We define this interface $x = S(t)$, as is common to phase-field problems of this class, as $r(S(t), t) = 1/2$. This is a compositional definition which is used in phase-change models (*e.g.* solidification, evaporation of a fluid). Another definition that is used in reacting fronts studies is that the location of the interface is where the medium achieves its critical temperature $\theta(S(t), t) = \theta_c$. We shall see in our numerical studies that these definitions are consistent, but that the speed of the moving interface may vary based on its definition [11]. To find the appropriate boundary conditions at this interface, we need to integrate the field equations (26)–(29) across a pillbox of size $\epsilon \gg \delta$ to find the appropriate jump conditions across the reaction region. We follow Anderson, McFadden and Wheeler [14] in this derivation, and we find the following interfacial conditions local to a moving frame $\xi = x - S(t)$:

$$\int_{-\epsilon}^{\epsilon}\left[\frac{\rho c_p(\phi)}{\rho c_p(0)}\theta\right]_t \mathrm{d}\xi - S'(t)\left[\frac{\rho c_p(\phi)}{\rho c_p(0)}\theta\right]\Bigg|_{-\epsilon}^{\epsilon} = \left[\frac{K(\phi)}{K(0)}\theta_\xi\right]\Bigg|_{-\epsilon}^{\epsilon}$$

$$+\int_{-\epsilon}^{\epsilon}\frac{K(\phi_0)}{K(0)}B\,P\,\frac{\zeta(\phi,\theta)}{\zeta(0,0)}|E|^2-2\mathcal{Q}r[1-\phi_0]^{r^2-1/4}\,C\,\mathrm{e}^{\frac{\mathcal{A}}{\delta}\left[\frac{1}{(\theta_c+1)}-\frac{1}{(\theta+1)}\right]}\mathrm{d}\xi\,, \quad (30)$$

$$\int_{-\epsilon}^{\epsilon}\left[r^2C\right]_t\mathrm{d}\xi-S'(t)\left[r^2C\right]\Big|_{-\epsilon}^{\epsilon}\;=\;\frac{\mathcal{D}}{\delta}\left[r^3\sqrt{\theta+1}C_\xi\right]\Big|_{-\epsilon}^{\epsilon}$$
$$-\frac{2}{\delta^2}\int_{-\epsilon}^{\epsilon}r\,C\,\mathrm{e}^{\frac{\mathcal{A}}{\delta}\left[\frac{1}{(\theta_c+1)}-\frac{1}{(\theta+1)}\right]}\mathrm{d}\xi\,, \quad (31)$$

$$\left[\frac{\mathrm{d}E}{\mathrm{d}x}\right]\Big|_{-\epsilon}^{\epsilon}+\int_{-\epsilon}^{\epsilon}k^2(\phi)\left[1+\mathrm{i}\nu(\phi)\right]E\mathrm{d}\xi\;=\;0\,, \quad (32)$$

$$\int_{-\epsilon}^{\epsilon}r_t\mathrm{d}\xi-S'(t)\,[r]\Big|_{-\epsilon}^{\epsilon}\;=\;-\mathcal{M}\int_{-\epsilon}^{\epsilon}C\,\mathrm{e}^{\frac{\mathcal{A}}{\delta}\left[\frac{1}{(\theta_c+1)}-\frac{1}{(\theta+1)}\right]}\mathrm{d}\xi\,, \quad (33)$$

where the notation $\left[f(\xi)\right]\Big|_{-\epsilon}^{\epsilon}=f(\epsilon)-f(-\epsilon)$.

In the limit $\epsilon\to 0$ with $0\ll\delta\ll\epsilon\ll 1$, we find that the integrals of the unsteady terms in Equations (30), (31), (33) vanish, since the quantities θ, r, C are expected to be bounded within the reaction region. By the same argument, and since E is expected to be bounded in the reaction region, the integrals involving the electric field E in Equations (30) and (32) also vanish in this limit. The only integral terms that do not vanish necessarily in the limit are those that involve the reaction term. To evaluate these integrals, the full problem within the pillbox $-\epsilon<\xi<\epsilon$ needs to be solved, through a matched asymptotic analysis to the solution of the problem outside of the reaction region, and then the integrals can be computed directly. However, we note that the assumption $\epsilon\gg\delta$ allows for the possibility of an asymptotic analysis of this integral. We defer this analysis to Appendix A, and for now assume that these reaction integrals can be computed in terms of the outer variables.

The conditions (30)–(32) are not sufficient to determine the appropriate boundary conditions at the interface. We augment these conditions with continuity of temperature and continuity of the electric field at the interface. The continuity of the electric field is a reasonable assumption since the reaction zone is very small compared to a wavelength. The choice of continuity of temperature is typically used in modeling exothermic reactions, where it is more likely that a jump in temperature across the reaction region is present compared to an endothermic reaction. Hence, our assumption is appropriate.

Thus, we have converted a single partial differential system (16)–(22) to two partial differential systems with interfacial conditions between the composite region $0<x<S$, where $r=C=\phi=0$, and the preform region $S<x<1$ where $r=1$, $\phi=\phi_0$. We can then write this system as, with $\tau=t\,\kappa(\phi_0)/\kappa(0)$,

$$\frac{\kappa(\phi_0)}{\kappa(0)}\theta_{2\tau}-\theta_{2xx}=\frac{K(\phi_0)}{K(0)}B\,P\,\frac{\zeta(0,\theta_2)}{\zeta(0,0)}|E_2|^2\,,\quad 0<x<S(\tau)\,, \quad (34)$$

$$\frac{\mathrm{d}^2E_2}{\mathrm{d}x^2}+k^2(0)\,[1+i\nu(0,\theta_2)]\,E_2=0\,, \quad (35)$$

$$\theta_{1\tau}-\theta_{1xx}\;=\;B\,P\,\frac{\zeta(\phi_0,\theta)}{\zeta(0,0)}|E_1|^2$$
$$-\frac{K(0)}{K(\phi_0)}\mathcal{Q}\left[1-\phi_0\right]^{-1/4}\,C\mathrm{e}^{\frac{\mathcal{A}}{\delta}\left[\frac{1}{\theta_c+1}-\frac{1}{\theta_1+1}\right]}\,,\quad S(\tau)<x<1\,, \quad (36)$$

$$\delta\frac{\kappa(\phi_0)}{\kappa(0)}C_\tau = \mathcal{D}\left[\sqrt{\theta_1+1}\,C_x\right]_x - \frac{1}{\delta}C\,\mathrm{e}^{\frac{\mathcal{A}}{\delta}\left[\frac{1}{\theta_c+1}-\frac{1}{\theta_1+1}\right]}\,, \tag{37}$$

$$\frac{\mathrm{d}^2E_1}{\mathrm{d}x^2} + k^2(\phi_0)\left[1+\mathrm{i}\nu(\phi_0,\theta_1)\right]E_1 = 0\,. \tag{38}$$

This system has to be solved with symmetry boundary conditions at $x = 0$,

$$\theta_{2x}(0,\tau) = 0\ ,\ \ E_2'(0) = 0\,, \tag{39}$$

the interfacial conditions at $x = S(t)$ given by

$$\theta_1(S,\tau) = \theta_2(S,\tau)\,, \tag{40}$$

$$\frac{K(\phi_0)}{K(0)}\theta_{1x} - \theta_{2x} = -\frac{\kappa(\phi_0)}{\kappa(0)}\,S'(\tau)\left\{\left(\frac{\rho c_p(\phi_0)}{\rho c_p(0)}-1\right)\theta_1(S,\tau)+\frac{\mathcal{Q}}{\mathcal{M}}\right\}\,, \tag{41}$$

$$E_1(S) = E_2(S)\,, \tag{42}$$

$$\frac{\mathrm{d}E_1}{\mathrm{d}x} = \frac{\mathrm{d}E_2}{\mathrm{d}x}\,, \tag{43}$$

$$\delta\mathcal{D}\sqrt{\theta_1(S,\tau)+1}\,C_x(S,\tau) = \frac{\kappa(\phi_0)}{\kappa(0)}\,S'(\tau)\left[\frac{1}{\mathcal{M}}-\delta^2\,C(S,\tau)\right]\,, \tag{44}$$

$$S'(\tau) = \frac{\kappa(0)}{\kappa(\phi_0)}\mathcal{M}\lim_{\epsilon\to 0}\int_{-\epsilon}^{\epsilon} C\mathrm{e}^{\frac{\mathcal{A}}{\delta}\left[\frac{1}{\theta_c+1}-\frac{1}{\theta_1+1}\right]}\mathrm{d}\xi\,. \tag{45}$$

At the preform/environment interface at $x = 1$, we find that

$$\theta_{1x} = -B\theta_1 - B\,R\left[(\theta_1+1)^4-1\right]\,,\quad C = 1\,. \tag{46}$$

2.3. The limit $\delta \to 0$

We now consider an asymptotic approach to the problem (34)–(46) in the limit $\delta \to 0$. We note that initially we assume that $\theta_1(x,0) = \theta_2(x,0) = 0$, and that $C(x,0) = 1$. With this assumption, we know that for a finite time the reaction terms in the energy and concentration equations for the preform will be exponentially small, compared to the algebraically small expansion below. Thus, we shall ignore these terms when solving the temperature and gas concentration within the preform. We need to monitor our solution for consistency with this assumption.

Following the analysis of the Pelesko and Kriegsmann [12] for the microwave heating problem, and motivated by the scales given in Table 1, we can define the ratio of thermal conductivites as

$$\frac{K(\phi_0)}{K(0)} = \gamma\delta\,,\quad \frac{\rho c_p(\phi_0)}{\rho c_p(0)} = \mu = O(1)\,, \tag{47}$$

and the ratio of electrical conductivities as

$$\frac{\zeta(0,\theta)}{\zeta(\phi_0,0)} = \frac{g(0,\theta)}{\delta^2}\,,\ \text{where } g(0,\theta) = \mathrm{e}^{3\theta}\,, \tag{48}$$

and expand each of the dependent variables in a regular asymptotic series in δ,

$$\theta_j = \theta_j^{(0)} + \delta\theta_j^{(1)} + \cdots , \tag{49}$$

$$C = C^{(0)} + \delta C^{(1)} + \cdots , \tag{50}$$

$$E_j = E_j^{(0)} + \delta E_j^{(1)} + \cdots . \tag{51}$$

At leading order we find in the composite $0 < x < S(t)$ that

$$\theta_{2xx}^{(0)} = 0 , \tag{52}$$

$$\frac{\mathrm{d}^2 E_2^{(0)}}{\mathrm{d}x^2} + k^2(0)\left[1 + \mathrm{i}\,\nu(0, \theta_2^{(0)})\right] E_2^{(0)} = 0 , \tag{53}$$

and in the preform $S(\tau) < x < 1$ that

$$\theta_{1\tau}^{(0)} = \theta_{1xx}^{(0)} , \tag{54}$$

$$\mathcal{D}\left[\sqrt{\theta_1^{(0)} + 1}\, C_x^{(0)}\right]_x = 0 , \tag{55}$$

$$\frac{\mathrm{d}^2 E_1^{(0)}}{\mathrm{d}x^2} + k^2(\phi_0) E_1^{(0)} = 0 . \tag{56}$$

Note that from (48) $\nu(\phi_0, 0) = O(\delta^2)$ if $\nu(0, 0) = O(1)$, resulting in the no-loss propagation of the electric field in the preform at this order. The boundary conditions at this order are the symmetry conditions

$$\theta_{2x}^{(0)} = E_{2x}^{(0)}(0) = 0, \tag{57}$$

and the interfacial conditions

$$\theta_1^{(0)}(S, \tau) = \theta_2^{(0)}(S, \tau) , \tag{58}$$

$$\theta_{2x}^{(0)} = 0 , \tag{59}$$

$$E_2^{(0)}(S) = E_1^{(0)}(S) , \tag{60}$$

$$E_{2x}^{(0)}(S) = E_{1x}^{(0)}(S) , \tag{61}$$

$$\left[\mathcal{D}\sqrt{\theta_1^{(0)}(S, \tau) + 1}\right] C_x^{(0)}(S, \tau) = \frac{\gamma}{\mu\, \mathcal{M}}\, S'(\tau) . \tag{62}$$

At the preform/environment interface we have

$$\theta_{1x}^{(0)} = -B\,\theta_1 - B\,R\left[(\theta_1^{(0)} + 1)^4 - 1\right], C = 1 . \tag{63}$$

Note that $\theta_2^{(0)}(x, \tau) = \theta_2^{(0)}(\tau)$. The electric field depends only parametrically in time, and following Pelesko and Kriegsmann [12], the resulting system for the temperature and gas concentration in the preform is

$$\theta_{1\tau}^{(0)} = \theta_{1xx}^{(0)} , \tag{64}$$

$$\left[\sqrt{\theta_1^{(0)} + 1}\; C_x^{(0)}\right]_x = 0 . \tag{65}$$

To determine the conservation of heat flux at the preform/composite interface $x = S(\tau)$, we integrate the $O(\delta)$ heat equation in the composite in x once across the composite, and noting

that there is zero heat flux at the line of symmetry $x = 0$, we arrive at the following boundary condition for $\theta_{1x}^{(0)}(S)$, along with the appropriate concentration flux boundary condition at $x = S(\tau)$,

$$\theta_{1x}^{(0)}(S,\tau) = \frac{S}{\mu}\theta_{1\tau}^{(0)} - B\,P\,\mathrm{e}^{3\,\theta_1^{(0)}}\int_0^S |E_2^{(0)}|^2\,\mathrm{d}x - \frac{1}{\mu}S'(\tau)\left\{(\mu-1)\,\theta_1^{(0)} + \frac{\mathcal{Q}}{\mathcal{M}}\right\}, \tag{66}$$

$$\left[\mathcal{D}\sqrt{\theta_1^{(0)}(S,\tau)+1}\right] C_x^{(0)}(S,\tau) = \frac{\gamma}{\mu\mathcal{M}}S'(\tau)\,. \tag{67}$$

At the preform/environment interface, we have

$$\theta_{1x}^{(0)} = -B\,\theta_1^{(0)} - B\,R\left[(\theta_1^{(0)}+1)^4 - 1\right],\ x = 1\quad, \tag{68}$$

$$C^{(0)} = 1\,. \tag{69}$$

In addition, from the analysis performed in Appendix A, the speed of the moving interface $S'(\tau)$ is, to leading order, given by

$$S'(\tau) = \begin{cases} 0, & \theta_1^{(0)}(S,\tau) < \theta_c \\ \dfrac{\mu\mathcal{M}(\theta_c+1)^2}{\gamma\mathcal{A}}\,C^{(0)}(S,\tau)\left\{\dfrac{\mathcal{A}}{(\theta_c+1)^2} - \dfrac{1}{\theta_{1x}^{(0)}(S,\tau)}\right\}, & \theta_1^{(0)}(S,\tau) = \theta_c \end{cases}. \tag{70}$$

This form has the restrictions that $\theta_1^{(0)} < \theta_c$ and $\theta_{1x}^{(0)} = o(\delta)$ for $x > S$. Note that the interfacial speed is dependent on the local gas concentration near the interface. This system requires initial conditions in τ for the temperature, concentration, and interfacial position $\theta_1^{(0)}(x,0) = \Theta_0(x)$, $C^{(0)}(x,0) = C_0(x)$, and $S(0) = S_0$.

A limitation in this process using conventional heating is that pores near the gas inlet may close prior to the the completion of the process. In Appendix B, we show in the asymptotic limit $\delta \to 0$ that inlet pore closure is equivalent to the condition $\theta_{1x}^{(0)} = O(\delta)$. Thus, we shall use this criterion in our numerical simulations below to terminate our calculation as the surface pores close and choke off the reactant from the physical process.

3. Results

We investigated the above system numerically for SiC deposited on an alumina preform. We scaled the moving domain $S(\tau) < x < 1$ to the stationary domain $0 < \xi < 1$, resulting in an advection-diffusion equation for temperature within the preform. Finite-difference techniques were used in space, and the updating in time was performed using Crank-Nicholson on the diffusion terms and upwinding on the advection terms. Since the gas concentration within the preform is quasi-steady, the solution could be found analytically for fixed time τ, and this analytic solution was implemented in the code for the solution to $C^{(0)}$. To avoid time-step errors when the reaction begins, the step function was modeled as a hyperbolic tangent function with some transition scale $q \ll \delta$. Typical values of q were in the range of 10^{-3}, and there was no quantitative change to this order in the solution for smaller values, provided that the time step was adjusted to resolve the transition to the reaction stage ($\Delta\tau = 10^{-5}$ in the results below). The numerical simulation was terminated when the asymptotic expansion

for $S'(\tau)$ ceased to be valid, or equivalently when the pore radius at the preform/environment interface $r(1, \tau)$ closed. We chose the condition that $\theta_{1x}^{(0)}(S, \tau) = 3\delta$ as the stopping criteria. Since this criterion is conservative, the completion-rate results presented below should be viewed as minimum completion rates. We address the dynamics of the process when this criterion is relaxed in the final section. To simplify in the presentation, we use the notation $\Theta = \theta_1^{(0)}$, $C = C^{(0)}$, and $E = E_2^{(0)}$. We further assume that the initial porosity $\phi_0 = 1/2$ in the results that follow.

A threshold power level is needed for the reaction to occur. If the interface remains fixed, then the system (37)–(43) yields a linear steady-state solution $\Theta(x, \tau) = \Theta_s(x)$, $S(\tau) = S_0$ subject to a nonlinear relation for the preform/composite interfacial temperature $\Theta_s(S_0)$ and the preform environment temperature $\Theta_s(1)$

$$\begin{aligned}\Theta_s'(x) &= -\frac{\Theta_s(S_0) - \Theta_s(1)}{1 - S_0} \\ &= -B\,P\,\mathrm{e}^{3\Theta_s(S_0)} \int_0^{S_0} |E(\Theta_s(S_0))|^2 \mathrm{d}x \\ &= -B\Theta_s(1) - B\,R\left[(\Theta_s(1) + 1)^4 - 1\right]. \end{aligned} \tag{71}$$

This relation shows that if the power parameter P is sufficiently weak, or if the initial substrate thickness is sufficiently small, then the steady interfacial temperature $\Theta_s(S_0)$ may never reach the critical temperature for the reaction to occur. We solve this nonlinear relation numerically for $S_0 = 0{\cdot}1$, $S_0 = 0{\cdot}5$, and $S_0 = 0{\cdot}9$ in Figure 2. Notice that for small initial powers that the steady-state solution remains below the required temperature Θ_c at which the reaction occurs. For larger power levels, the only steady-state solution is represented by the upper branch, where the skin effect within the composite limits its absorption of power. Note that for thicker initial composites, the required power needed to instigate the transition to the upper branch is less [12, 16].

In Figure 3 we show the temperatures at the preform/composite interface with $P = 0{\cdot}1, 0{\cdot}2, 0{\cdot}3, 0{\cdot}4$ and $S_0 = 0{\cdot}1$, based on our time-dependent numerical solution of (37)-(43) without reaction. In the cases $P = 0{\cdot}1, 0{\cdot}2, 0{\cdot}3$, the temperature attains a steady state, since the power generated by the microwaves balance the heat loss at the preform/environment interface. This heat loss is not sufficient for the case $P = 0{\cdot}4$. The steady state occurs on the upper branch where the skin-effect mechanism limits further growth [16]. This is not shown in Figure 3. The steady-state results are identical to those given by the S-shaped response curve in Figure 2. For all the cases considered, the values of equilibrium temperature along the upper branch of the S-shaped curve are larger than the critical temperature at which the reaction takes place.

We now focus our attention on the dynamical problem where the boundary is allowed to propagate. There are three distinct stages of the time-dependent process that we can identify. Firstly, there is the inert heating stage, when the substrate is heated by the microwaves and the preform by thermal diffusion. No reaction occurs during this stage. The second régime is the processing stage where the temperature at the preform/composite interface is at Θ_c, and interface $S(\tau)$ begins to move to the right. The final stage occurs when the reaction front is close enough to the preform/environment interface to produce a nearly uniform temperature. This implies that the temperature of the preform is near the critical temperature: the pores close quickly on a time scale commensurate with the front propagation. During this third stage our reaction assumption is violated and its resolution can only be found by solving the

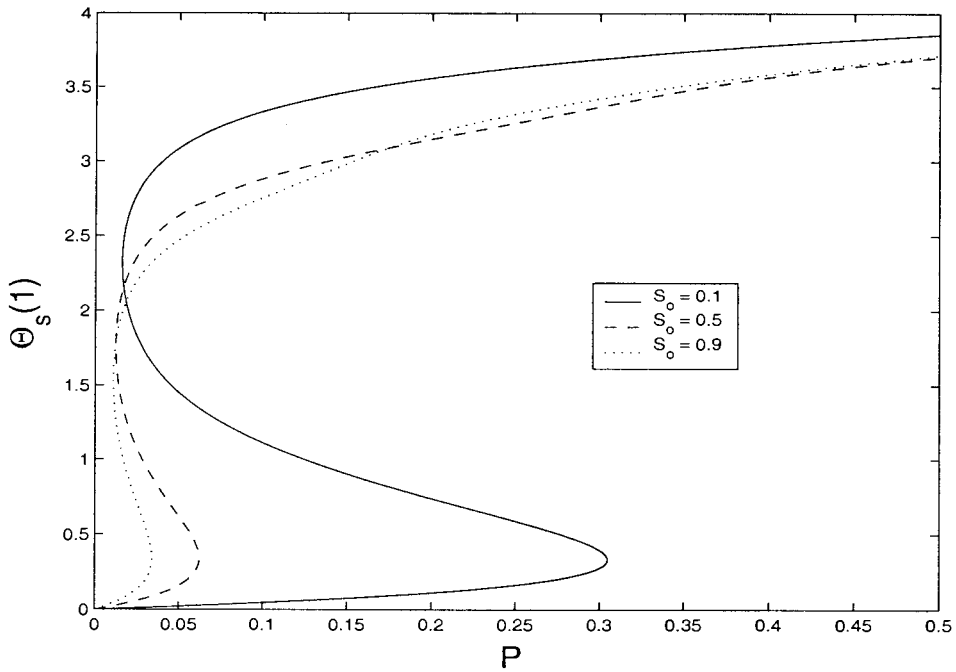

Figure 2. Steady-state preform/environment temperatures $\Theta_s(1)$ plotted against input power P for $S_0 = 0{\cdot}1$, $S_0 = 0{\cdot}5$ and $S_0 = 0{\cdot}9$. In all the cases, power levels above $P = 0{\cdot}3049$ will result in the solution represented by the upper branch.

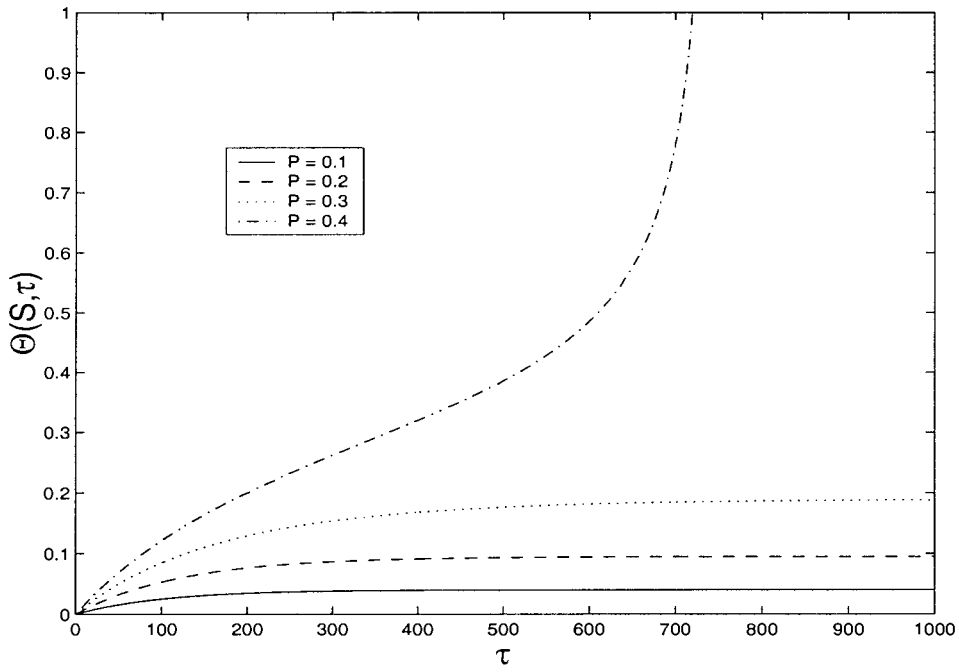

Figure 3. Composite/preform interfacial temperature as a function of τ for different power levels $P = 0{\cdot}1, 0{\cdot}2, 0{\cdot}3, 0{\cdot}4$ with $S_0 = 0{\cdot}1$. We see that for sufficiently small power levels, the system achieves a lower-branch steady state. $P = 0{\cdot}4$ shows the transition to the upper branch.

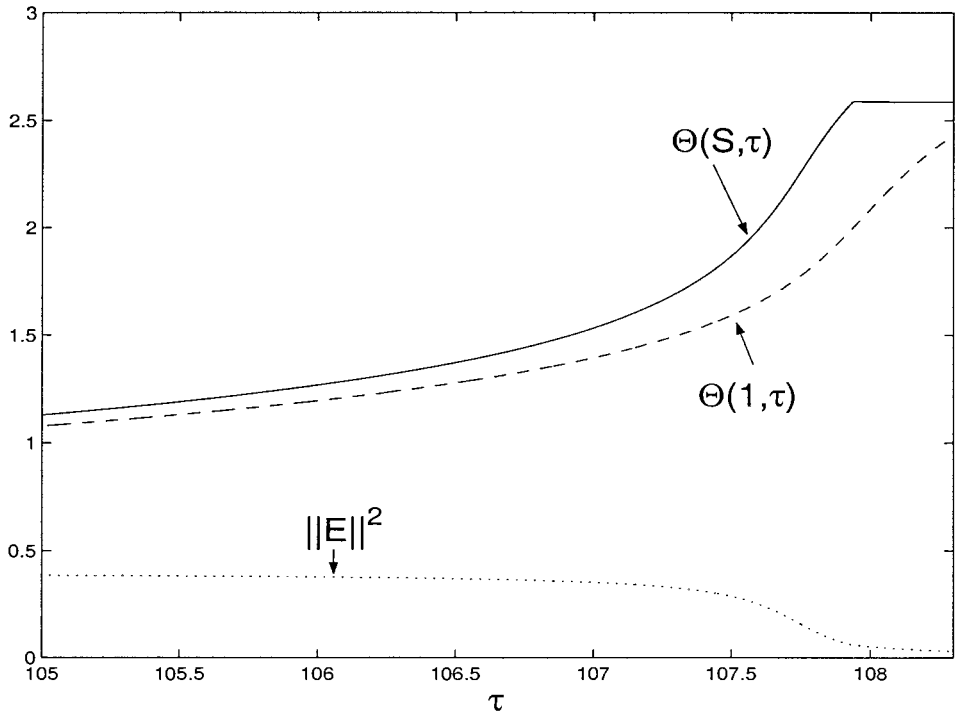

Figure 4. Composite interfacial temperature $\Theta(S, \tau)$, preform/environment interfacial temperature $\Theta(1, \tau)$, and the integral of the electric-field amplitude in the composite $||E(S, \tau)||^2 = \int_0^S |E(x, \tau)|^2 dx$ as a function of τ for $P = \mathcal{M} = 1$, $\Theta(x, 0) = 0$. We see from times $\tau = 0$ (not shown) to $\tau = 107{\cdot}95$ that the system is being heated due to the microwaves. The onset of thermal runaway is seen in the decrease in the magnetic field due to the skin effect within the composite. The composite interfacial temperature is essentially fixed at Θ_c during the process.

original phase-field type system in the reduced domain $S(\tau) < x < 1$. We do not address this case here.

We begin by considering the particular case $P = 1$, $S_0 = 0{\cdot}1$. When the initial pore radius is $r_0 = 1\mu$m and the sample size $a = 1$ cm, then $P = 1$ corresponds to a power density of approximately 30 W/cm^2, and $\tau = 100$ corresponds to a time of 1.85 hours. In all of the simulations that follow, we assume that the remaining physical parameters are fixed: $\mathcal{A} = 1$, $\mathcal{D} = 0{\cdot}6$, $k(0) = \nu(0, 0) = 0{\cdot}1$, and $k(\phi_0) = 0{\cdot}15$. In Figure 4, we show the temperatures $\Theta(S, \tau)$ and $\Theta(1, \tau)$ as a function of the time τ over the process, in addition to the integral of the magnitude of the electric field at the preform/composite interface $||E(S, \tau)||^2$. We see that during the inert stage the temperature increases up to the critical temperature and the electric field in the substrate is essentially constant. Prior to reaching the critical temperature, the interfacial temperature appears to be in thermal runaway with the amplitude of the electric field decreasing. This feature is consistent with the skin effect occurring in the composite. In the processing stage, the temperature remains fixed at Θ_c, and the magnitude of the electric field decays as the domain of the composite increases with $S(\tau)$. This process continues until the temperature in the preform is, based on our stopping criterion, nearly spatially uniform.

In Figure 5 we show the evolution of the concentration at the composite/preform interface $C(S, \tau)$ as a function of τ. Note that once the reaction begins, there is an immediate loss of concentration, which then relaxes as $S(\tau)$ moves into the preform. The discontinuity at the onset of the reaction can be resolved by reintroducing the time derivative in Equation (65).

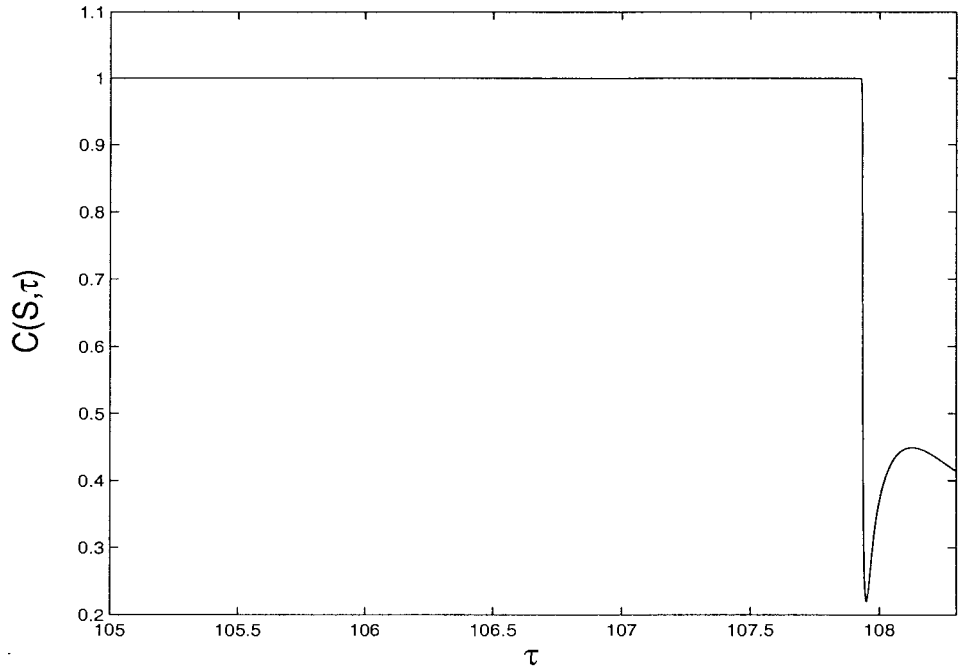

Figure 5. Preform gas concentration $C(S, \tau)$, as a function of τ for $P = \mathcal{M} = 1$, $\Theta(x, 0) = 0$. After the process begins, there is an immediate depletion of the gas local to the composite interface.

Figure 6 shows the evolution of the interfacial location $S(\tau)$ over time, and we note that the rate of growth slowly increases during the process. This weak effect occurs because the temperature gradient in the preform is becoming more shallow, as seen from Equation (70).

The temperature and concentration profiles are shown in Figures 7 and 8, respectively. Note that as the composite grows into the preform, the preform temperature becomes more uniform. This effect causes the concentration to be nearly linear, as can be easily deduced by integrating equation (65).

There are three control parameters that can be used either to enhance the final composition percentage of the system or to shorten the processing time: P, $\mathcal{M}$ and $\Theta_0 = \Theta(x, 0)$.

In Figure 9, we show the final interfacial location for different values of P given the initial composition thicknesses $S_0 = 0{\cdot}1, 0{\cdot}2, 0{\cdot}3, 0{\cdot}5$. We see that the final interfacial positions S_f do not depend on the initial composite thickness, but are improved with increased power. Figure 10 shows the values τ_f at which the simulation is terminated. Note that increasing the initial thickness S_0 shortens the processing time, as is expected. In addition, increasing the power, for a fixed S_0, reduces τ_f. Figure 11 shows the final position S_f as a function of the mass ratio $\mathcal{M}$ for an input power of $P = 1$. Notice that there is a limiting final composition that is possible, no matter how large the gas concentration parameter $\mathcal{M}$ becomes. In addition, the final time τ_f is independent of $\mathcal{M}$ in this parameter range as well. This can be inferred from Equations (39) and (40), where we notice that the the concentration flux and the jump in the temperature flux at $x = S(\tau)$ are independent of $\mathcal{M}$. For sufficiently slow propagation speeds $S'(\tau)$, corresponding to small $\mathcal{M}$, heat transport across the preform is faster than the front propagation, leading to a poor final composite fraction.

A more curious effect is how the initial ambient temperature can affect the process. There is little dependence on the final composition as a function of initial temperature Θ_0, where $S_f =$

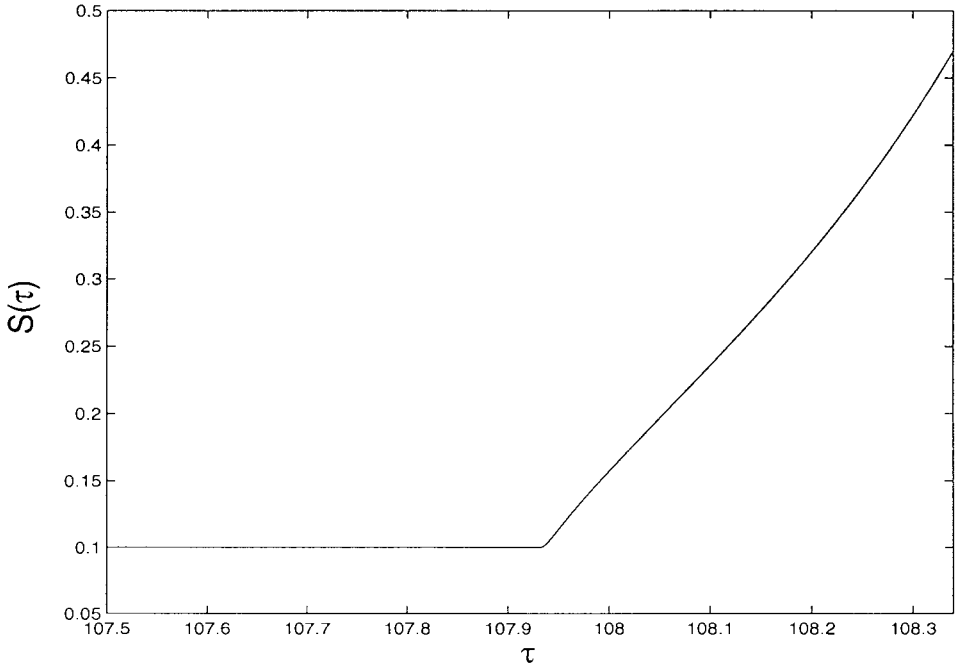

Figure 6. Composite interfacial location $S(\tau)$, as a function of τ for $P = \mathcal{M} = 1$, $\Theta(x, 0) = 0$.

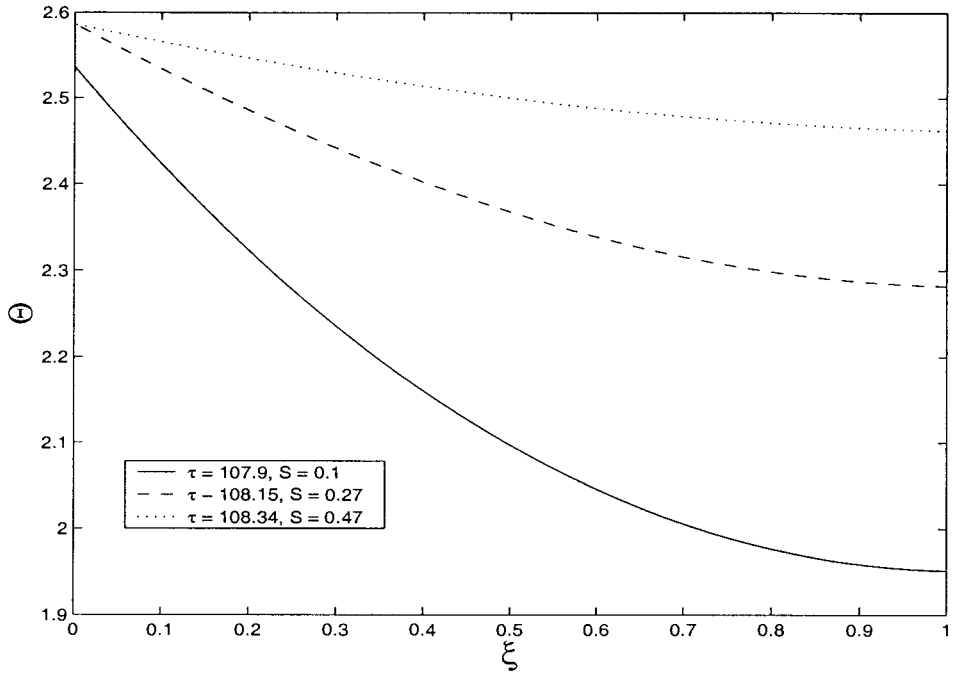

Figure 7. Preform temperature profiles at the values $\tau = 107{\cdot}9$, $S(\tau) = 0{\cdot}1$, $\tau = 108{\cdot}15$, $S(\tau) = 0{\cdot}27$ and $\tau = 108{\cdot}34$, $S(\tau) = 0{\cdot}47$ for $P = \mathcal{M} = 1$, $\Theta(x, 0) = 0$. Note that these plots are in the scaled domain $\xi = (x - S(\tau))/(1 - S(\tau))$.

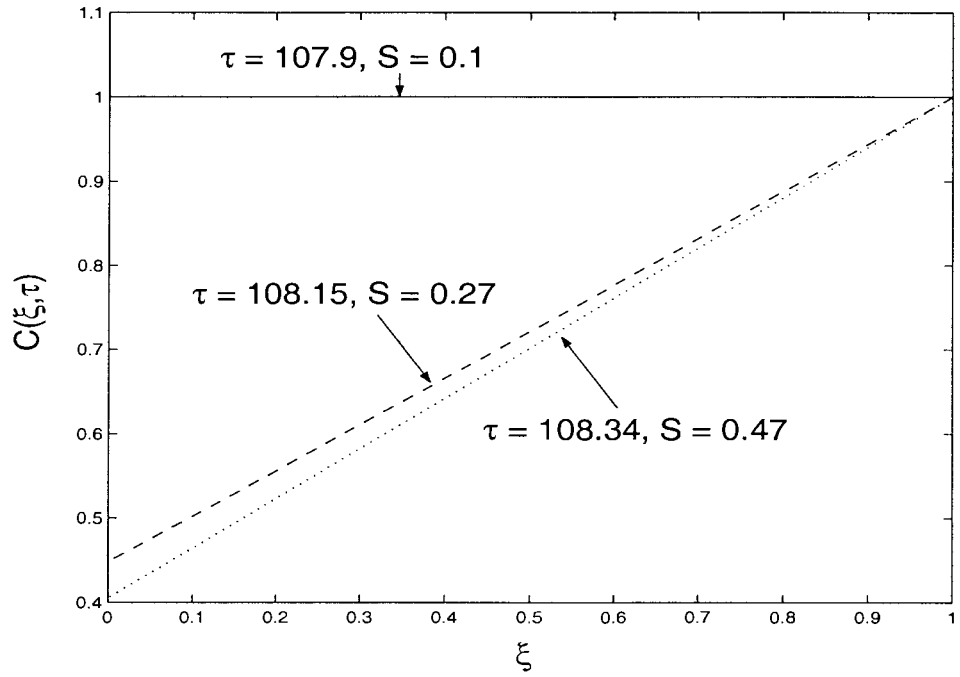

Figure 8. Gas concentration profiles at the values $\tau = 107{\cdot}9$, $S(\tau) = 0{\cdot}1$, $\tau = 108{\cdot}15$, $S(\tau) = 0{\cdot}27$ and $\tau = 108{\cdot}34$, $S(\tau) = 0{\cdot}47$ for $P = \mathcal{M} = 1$, $\Theta(x, 0) = 0$. Note that these plots are in the scaled domain $\xi = (x - S(\tau))/(1 - S(\tau))$. The profiles are nearly linear, since the gradients in temperature seen in Figure 7 are small.

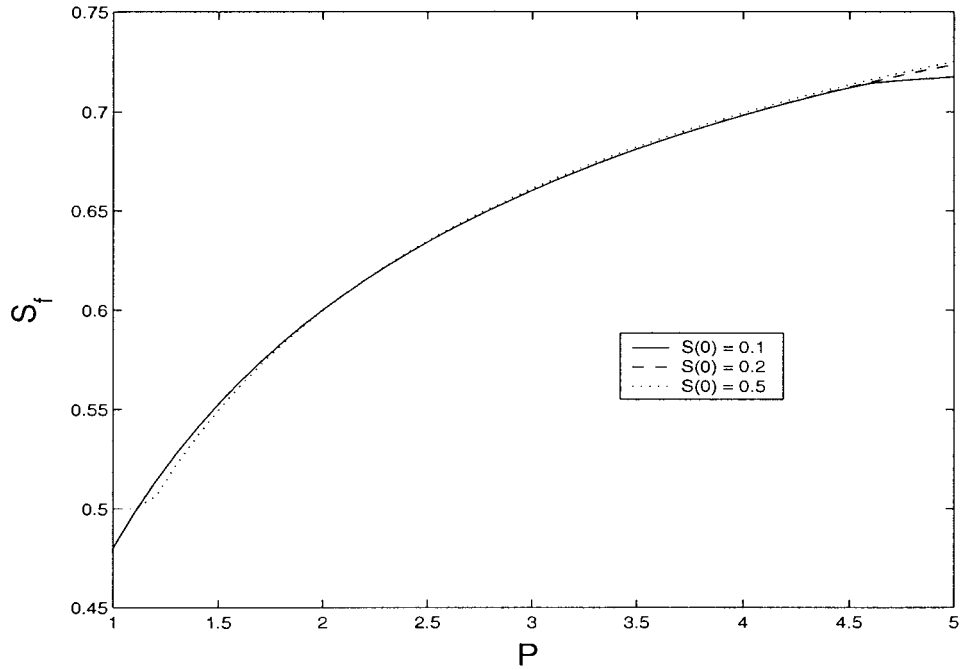

Figure 9. Final interfacial locations S_f for different input power levels with $\mathcal{M} = 1$, $\Theta_0 = 0$ and initial composite thicknesses $S(0) = 0{\cdot}1$, $S(0) = 0{\cdot}2$, and $S(0) = 0{\cdot}5$. Larger input powers lead to better completion.

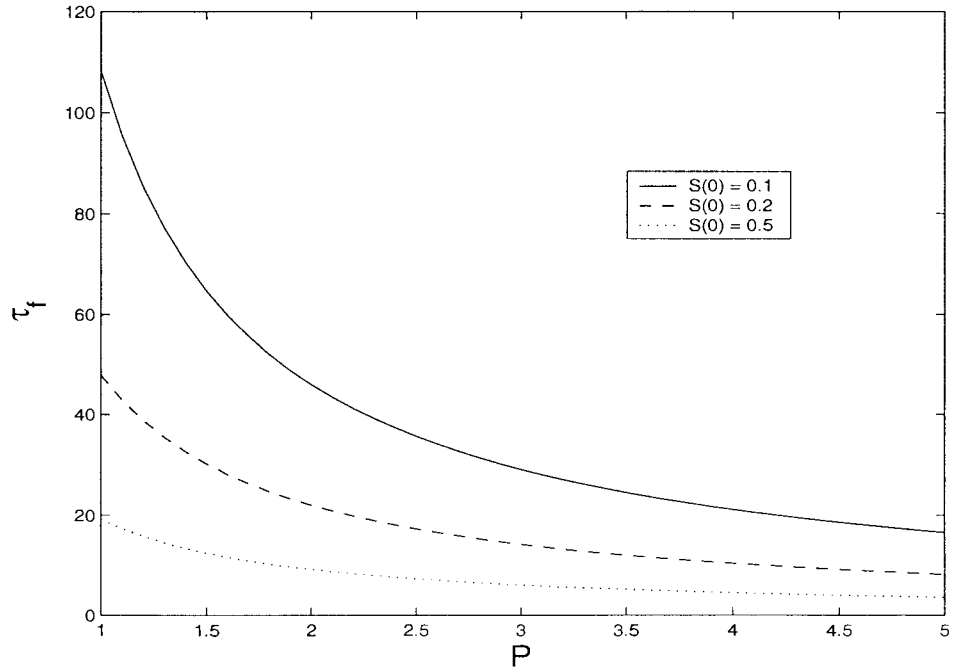

Figure 10. Final processing times for different input power levels for $\mathcal{M} = 1$, $\Theta_0 = 0$, and initial composite thicknesses $S(0) = 0{\cdot}1$, $S(0) = 0{\cdot}2$, and $S(0) = 0{\cdot}5$. Larger input powers lead to faster rates of completion.

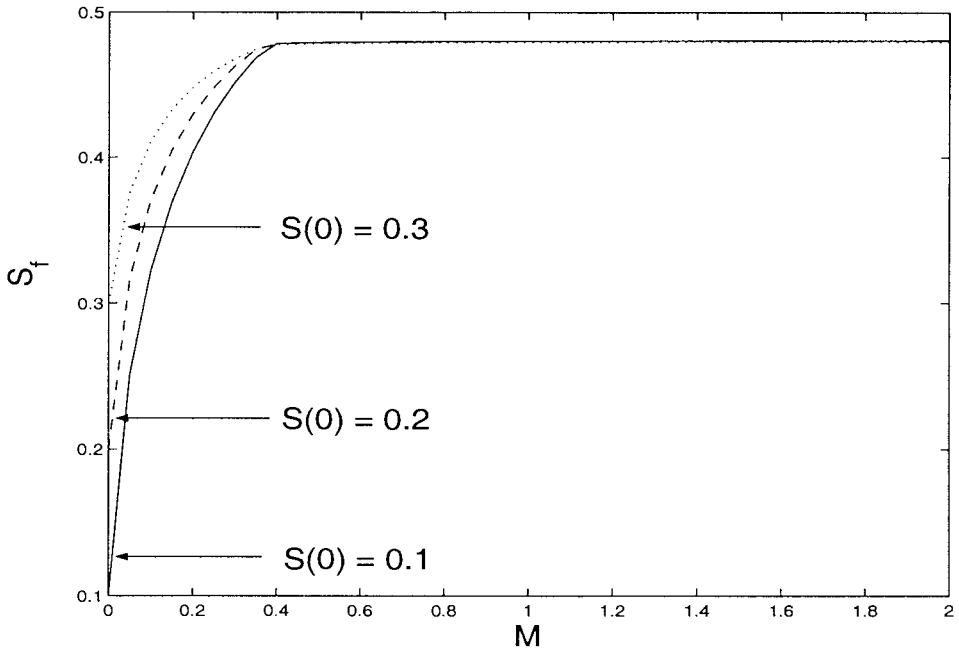

Figure 11. Final interfacial locations S_f for different inlet gas concentrations $\mathcal{M}$ for $P = 1$, $\Theta_0 = 0$, and initial composite thicknesses $S(0) = 0{\cdot}1$, $S(0) = 0{\cdot}2$. We see that there is a critical value of $\mathcal{M}$ above which the final composition is minimally affected. Note that in the $S(0) = 0{\cdot}2$ case that there is a detrimental effect of larger gas concentrations to the final composition fraction.

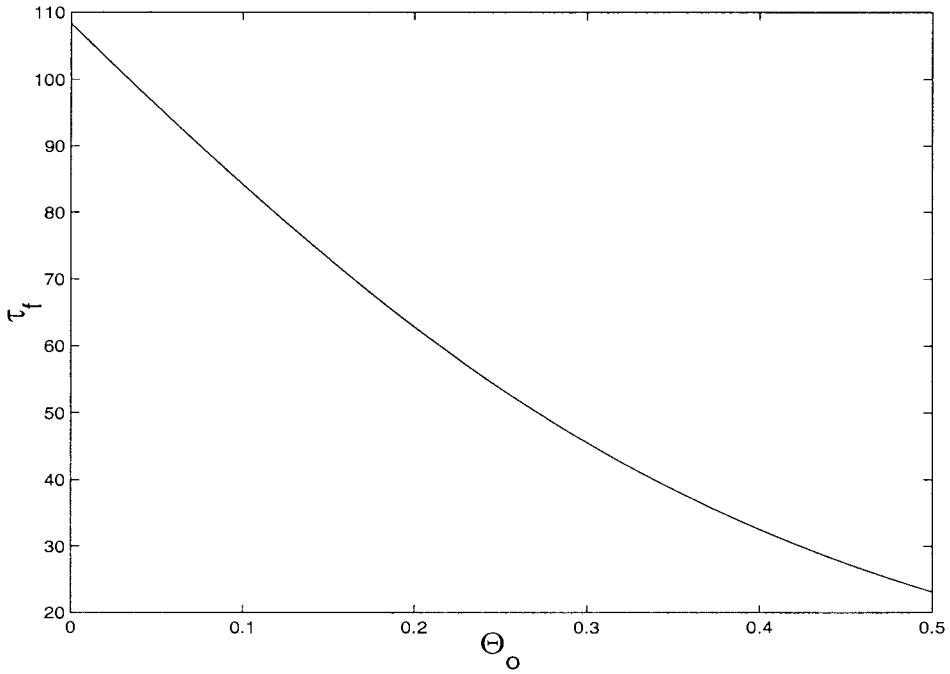

Figure 12. Sensitivity of the processing time τ_f to the initial ambient temperature Θ_0 for $P = \mathcal{M} = 1$.

0·47 for $0 < \Theta_0 < 0{\cdot}5$ for $P = \mathcal{M} = 1$. However, the processing times τ_f vary significantly over the same domain, even for small increases in temperature as is shown in Figure 12. The driving factor is the strong dependence of electrical conductivity on temperature. For elevated temperatures, the composite heats up more quickly, while the rate of heat transport in the preform is unaffected. Thus, the same final composition is achieved in a shorter time. Clearly, more overall energy needs to be expended in this case.

4. Conclusions

We have investigated a simple model of microwave-enhanced chemical vapor infiltration using the decomposition of TMS as a paradigm. By using the large activation-energy limit, we derived a sharp interface model which describes the motion of a moving front that separates the composite from the preform. This model takes into account the effects of changing material properties during the process, the heat of reaction, and nonuniformities in the gas concentration within the preform. This model is most useful in the limit where the time-scale of the reaction is much shorter than that of thermal conduction within the preform.

In a previous work [11], we used a thermally based definition of the interfacial location, assuming that variations in gas concentration were negligible. From our analysis in Appendix B, we find that the definition used in that work and the compositional definition used here differ by $O(\delta)$. Thus, if concentration gradients are assumed to be neglible, then these two definitions of the interfacial location are reconciled. However, with a spatially dependent gas concentration field, the thermally-based definition is not appropriate.

A second comment relates to our conservative choice of the termination criterion for our simulation. The asymptotic analysis gives a scale at which the asymptotics are no longer

valid $\Theta_x(S,\tau) = O(\delta)$. There is some freedom in the choice of quantitatively interpreting this condition. The choice used in this work is considered conservative. However, we did continue the run presented in Figure 4 until $\Theta_x(S,\tau) = 0{\cdot}25\,\delta$. In that case, we found that the final compositional value $S_f = 0{\cdot}77$, a 60% improvement over the case used in the paper. Occasionally, asymptotic models can be useful even beyond their range of asymptotic validity. A full solution to the original porous problem would have to be undertaken to determine the accuracy of the asymptotic model presented here beyond its range of validity.

Since the model is based on a sharp interface between the composite and the preform, higher dimensional extensions can be formulated in a straightforward manner. In addition, the presence of HCl gas within the preform as the system reacts is detrimental to the composition process. Including this effect, in addition to a forced flow in the *y*-direction can also be implemented using the presented theory relatively directly. Finally, we note that this model does not include the possibility of the microwave heating of the preform. Such considerations will be the subject of future works.

Acknowledgements

This work was supported by a grant from the National Science Foundation (DMS-9971383) (BST), by a grant from the US Department of Energy (DE-FG02-94ER25196) (GAK) and by a grant from the National Science Foundation (DMS 0071368) (GAK).

Appendix A

In this section, we derive the asymptotic expansion of integrals of the form

$$I = \int_{-\epsilon}^{\epsilon} F(r) C \mathrm{e}^{\frac{\mathcal{A}}{\delta}\left[\frac{1}{\theta_c+1} - \frac{1}{\theta+1}\right]} \mathrm{d}\xi \,, \tag{A1}$$

in the limit where $0 \ll \delta \ll \epsilon$. Firstly, we can use the mean-value theorem for integrals to eliminate the dependence on the cylinder radius r,

$$I = F(\hat{r}) \int_{-\epsilon}^{\epsilon} C \mathrm{e}^{\frac{\mathcal{A}}{\delta}\left[\frac{1}{\theta_c+1} - \frac{1}{\theta+1}\right]} \mathrm{d}\xi \tag{A2}$$

where $0 < \hat{r} < 1$. In the limit as $\epsilon \to 0$, we find that $\hat{r} \to 1/2$. The remainder of the integral is determined based on the assumption that $C(\xi,t) = 0$ if $-\epsilon < \xi < -\delta$, that is, there is no gas concentration within the composite. With the ansatz, the integral I can be decomposed into two different integrals,

$$\begin{aligned} I &= I_+ + I_- \\ &= \int_0^{\epsilon} C \mathrm{e}^{\frac{\mathcal{A}}{\delta}\left[\frac{1}{\theta_c+1} - \frac{1}{\theta+1}\right]} \mathrm{d}\xi + \int_{-\delta}^{0} C \mathrm{e}^{\frac{\mathcal{A}}{\delta}\left[\frac{1}{\theta_c+1} - \frac{1}{\theta+1}\right]} \mathrm{d}\xi \,. \end{aligned} \tag{A3}$$

Standard asymptotic techniques (*e.g.* Laplace's method [15]) can be applied after the substitution $u = \xi/\delta$ is made. From this expansion, and noting that $\epsilon/\delta \to \infty$, we find that for $\theta(S,t) = \theta_c$

$$I_+ = -C(S,t) \left\{ \frac{\delta\,[\theta_c + 1]^2}{\mathcal{A}\theta_x^+(S,t)} \right\} + O(\delta^2) \,, \tag{A4}$$

$$I_- \;=\; C(S,t)\left\{\frac{\delta\,[\theta_c+1]^2}{\mathcal{A}\theta_x^-(S,t)}\right\}\left(1-\exp\left[\frac{-\mathcal{A}\theta_x^-(S,t)}{(\theta_c+1)^2}\right]\right)+O(\delta^2)\,, \tag{A5}$$

where the expansion for I_- breaks down when $\theta_x^-(S,t)=O(\delta)$.

Appendix B

In this section, we derive the time for the inlet pore to close at $x=1$, given the temperature variation in time. Consider

$$\frac{\partial r}{\partial \tau} \;=\; -\frac{\mathcal{M}}{\delta}\,C(1,\tau)\mathrm{e}^{\frac{\mathcal{A}}{\delta}\left[\frac{1}{\theta_c+1}-\frac{1}{\theta_1(1,\tau)+1}\right]}\,, \tag{B1}$$

with the initial condition $r(1,\tau)=1$. we can formally integrate this in time

$$r(1,\tau) \;=\; 1-\mathcal{M}\int_0^{\tau} C(1,\tau)\mathrm{e}^{\frac{\mathcal{A}}{\delta}\left[\frac{1}{\theta_c+1}-\frac{1}{\theta_1(1,\tau)+1}\right]}\frac{\mathrm{d}\tau}{\delta}\,. \tag{B2}$$

Let us define τ_c as the time at which $\theta_1(1,\tau_c)=\theta_c$. Then, in the limit $\delta\to 0$, the integrand is exponentially small provided that $\theta_1(1,\tau)-\theta_c\gg\delta$. If we chose then some value $\Delta\tau\gg\delta$, then we can write the pore radius as

$$r(1,\tau) \;=\; \begin{cases} 1-\mathcal{M}\displaystyle\int_{\tau_c-\Delta\tau}^{\tau} C(1,\tau)\mathrm{e}^{\frac{\mathcal{A}}{\delta}\left[\frac{1}{\theta_c+1}-\frac{1}{\theta_1(1,\tau)+1}\right]}\frac{\mathrm{d}\tau}{\delta} & \tau>\tau_c-\Delta\tau \\ 1 & \tau<\tau_c-\Delta\tau \end{cases}\,. \tag{B3}$$

Note that since we are restricting our analysis to $x=1$, $C(1,\tau)=1$ for all τ.

If $0<\delta\ll\Delta\tau\ll 1$, then we can expand the temperature $\theta_1(1,\tau)$ as a power series of $\tau-\tau_c=\delta u$,

$$\theta_1(1,\tau)=\theta_c+\delta u\theta_{1\tau}(1,\tau_c)+\ldots$$

and rewrite the integral for the pore radius as

$$r(1,\tau) \;=\; \begin{cases} 1-\mathcal{M}\int_{-\Delta\tau/\delta}^{u}\mathrm{e}^{\frac{\mathcal{A}}{\delta}\left[\frac{\theta_c'\delta u+O(\delta^2)}{(\theta_c+1)(\theta_c+\delta\theta_c' u+O(\delta^2))}\right]}\mathrm{d}u & \tau>\tau_c-\Delta\tau \\ 1 & \tau<\tau_c-\Delta\tau \end{cases}\,, \tag{B4}$$

where $\theta_c'=\theta_{1\tau}(1,\tau_c)$. If we define the time τ_f as the time when the pore closes, then the corresponding time u_f obeys to leading order

$$\mathcal{M}\frac{[\theta_c+1]^2}{\mathcal{A}\theta_c'}\exp\left[\frac{\mathcal{A}\,\theta_c' u_f}{[\theta_c+1]^2}\right] \;=\; 1\,. \tag{B5}$$

From this, we find that the time for the pore to close τ_f is given by

$$\tau_f \;=\; \tau_c+\delta\frac{[\theta_c+1]^2}{\mathcal{A}\theta_c'}\log\left[\frac{\mathcal{A}\theta_c'}{\mathcal{M}[\theta_c+1]^2}\right]. \tag{B6}$$

Thus, the pore closure time is within $O(\delta)$ of the time at which the temperature $\theta_1(1,\tau)=\theta_c$. Since we find that temperature variations in time are $O(1)$ late in the process, and the temperature $\theta_1(x,\tau)$ is monotonically decreasing in x, then this can only happen when $\theta_1(S,\tau)-\theta_1(1,\tau)=O(\delta)$, or when $\theta_{1x}(S,\tau)=O(\delta)$.

References

1. T. L. Starr and A. W. Smith, 3-D modeling of forced-flow thermal-gradient CVI for ceramic composite fabrication. *Materials Research Special Symposium* 168 (1990).
2. A. Ditkowski, D. Gottleib, and B. W. Sheldon, On the mathematical analysis and optimization of chemical vapor infiltration in materials science. *Mathematical Modeling and Numerical Analysis* 40 (2000) 337–351.
3. D. Jaglin and J. Binner, Densification of woven fibre SiC/SiC composites by microwave enhanced chemical vapor infiltration. *7th Int. Conf. Microwave and High Frequency Heating* (1999) pp. 283–286.
4. S. V. Sotirchos, Dynamic modeling of chemical vapor infiltration, *AIChE J.* 37 (1991) 1365–1378.
5. D. Gupta and J. W. Evans, A mathematical model for chemical vapor infiltration with microwave heating and external cooling, *J. Materials Res.* 40 (1991) 810–818.
6. D. Gupta and J. W. Evans, Calculation of temperatures in microwave-heated two-dimensional ceramic bodies, *J. Amer. Ceramic Soc.* 76 (1993) 1915–1923.
7. D. Gupta and J. W. Evans, Mathematical model for chemical vapor infiltration in a microwave-heated preform, *J. Amer. Ceramic Soc.* 76 (1993) 1924–1929.
8. B. J. Matkowsky and G. I. Sivashinsky, Propagation of a pulsating reaction front in solid fuel combustion. *SIAM J. Appl Math.* 35 (1978) 465–478.
9. B. J. Matkowsky and G. I. Sivashinsky, An asymptotic derivation of two models in flame theory associated with the constant density approximation *SIAM J. Appl. Math.* 37 (1979) 686–699.
10. S. B. Margolis, An asymptotic theory of heterogenous condensed combustion *Combust. Sci. Tech.* 43 (1985) 197–215.
11. B. S. Tilley and G. A. Kriegsmann, Microwave-enhanced chemical vapor infiltration: a moving interface model. *Second World Congress on Microwave and Radio-Frequency Processing* (to appear).
12. J. A. Pelesko and G. A. Kriegsmann, Microwave heating of ceramic laminates, *J. Eng. Math.* 32 (1997) 1–18.
13. D. J. Skamser, J. T. Thomas, H. M. Jennings and D. L. Johnson, A model for microwave processing of compositionally changing ceramic systems *J. Materials Res.* 10 (1995) 3160–3178.
14. D. M. Anderson, G. B. McFadden and A. A. Wheeler, Diffuse-interface methods in fluid mechanics. *Ann. Rev. Fluid Mech.* 30 (1998) 139–165.
15. C. M. Bender and S. A. Orszag, *Advanced Mathematical Methods for Scientists and Engineers*. International Series in Pure and Applied Mathematics. New York: McGraw-Hill Book Company (1978) 593 pp.
16. G. A. Kriegsmann, Thermal runaway in microwave heated ceramics: a one-dimensional model *J. Appl. Phys.* 71 (1992) 1960–1966.